# CRYSTAL GROWTH & DESIGN

X-ray Transparent Microfluidic Chip for Mesophase-Based Crystallization of Membrane Proteins and On-Chip Structure Determination

Daria S. Khvostichenko,[†,§] Jeremy M. Schieferstein,[†,§] Ashtamurthy S. Pawate,[†] Philip D. Laible,[‡] and Paul J. A. Kenis*,[†]

[†]Department of Chemical & Biomolecular Engineering, University of Illinois at Urbana−Champaign, 600 South Mathews Avenue, Urbana, Illinois 61801, United States

[‡]Biosciences Division, Argonne National Laboratory, Argonne, Illinois 60439, United States

Ⓢ Supporting Information
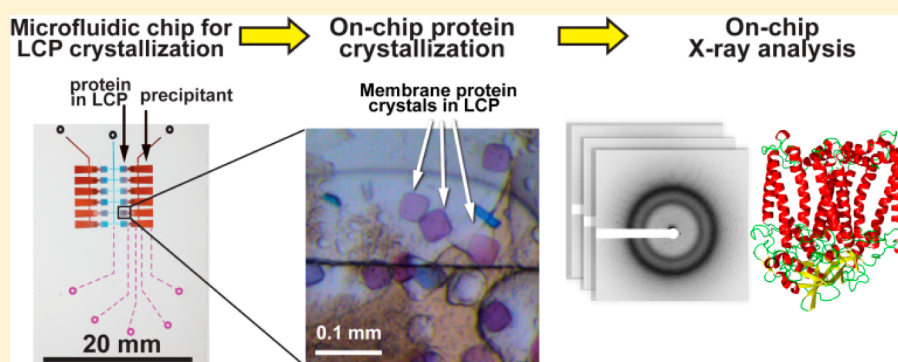
ABSTRACT: Crystallization from lipidic mesophase matrices is a promising route to diffraction-quality crystals and structures of membrane proteins. The microfluidic approach reported here eliminates two bottlenecks of the standard mesophase-based crystallization protocols: (i) manual preparation of viscous mesophases and (ii) manual harvesting of often small and fragile protein crystals. In the approach reported here, protein-loaded mesophases are formulated in an X-ray transparent microfluidic chip using only 60 nL of the protein solution per crystallization trial. The X-ray transparency of the chip enables diffraction data collection from multiple crystals residing in microfluidic wells, eliminating the normally required manual harvesting and mounting of individual crystals. We validated our approach by on-chip crystallization of photosynthetic reaction center, a membrane protein from *Rhodobacter sphaeroides*, followed by solving its structure to a resolution of 2.5 Å using X-ray diffraction data collected on-chip under ambient conditions. A moderate conformational change in hydrophilic chains of the protein was observed when comparing the on-chip, room temperature structure with known structures for which data were acquired under cryogenic conditions.

Integral membrane proteins are of paramount importance in the regulation of physiological processes in the cell, and consequentially, they account for over 60% of all drug targets known to date.[1] However, crystal structures of membrane proteins, the primary source for atomic-level information on their functional mechanisms, are only scarcely available compared to soluble proteins. This disparity originates in part in the inherent amphiphilicity of membrane proteins that limits their solubility and stability in aqueous solutions even in the presence of solubilizing detergents, leading to a very low success rate of crystallization efforts.

A powerful alternative to crystallization from solutions has emerged in recent years where membrane proteins are crystallized from lipidic cubic phases (LCP),[2] leading to structural determination of several important proteins from the GPCR family.[3] In the LCP method, membrane proteins are embedded in a lipidic mesophase matrix that mimics a native lipid bilayer environment throughout the crystallization process.[2] The mesophases form spontaneously when aqueous solutions are mixed with certain lipids, typically of the monoacylglycerol family,[4] to form different bilayer phases.[5] As in other protein crystallization approaches, the success of the LCP method relies on screening a large number of crystallization conditions,[2,6] which is difficult due to the high viscosity and stickiness of lipidic mesophases and requires specialized tools that make handling many samples cumbersome.[2,7] Automated screening approaches and novel crystallization protocols alleviate some of these problems,[7,8] but harvesting of protein crystals from mesophases is still performed manually. Harvested crystals are cooled in liquid
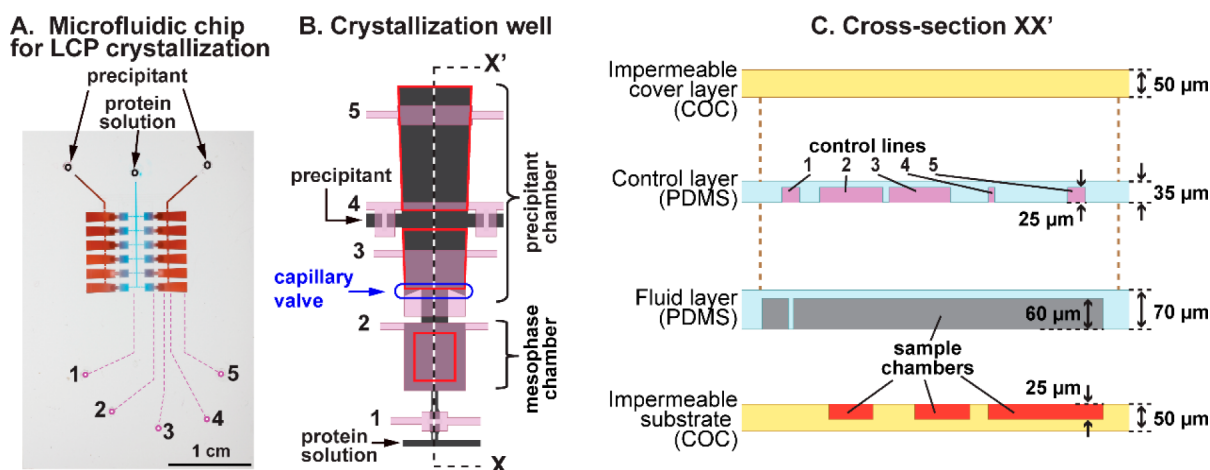
Figure 1. (A) Photograph of the 2 × 6-well array chip. Lilac dotted lines (1−5) indicate the different control lines connected to control valves. (B) Magnified top view schematic of a single crystallization well comprising three patterned layers and a top unpatterned COC layer: first layer (PDMS, lilac) contains control lines and valves, and second (PDMS, black) and third (COC, red outlines) layers contain sample compartments. (C) Cross section of a crystallization well showing the layered assembly of the chip.

nitrogen and maintained under cryogenic conditions to prevent radiation damage and dehydration during data collection.[7] The typically small size, 2−70 μm,[6] of membrane protein crystals makes this procedure highly challenging. The damage caused to the delicate crystals in this step may severely compromise the quality of resulting structures.

Numerous examples of microfluidic technologies that automate fluid metering and drastically reduce sample consumption have been demonstrated for protein crystallization from solutions.[9] Furthermore, a number of X-ray transparent microfluidic devices that eliminate manual crystal handling are available.[10] In contrast, only two microfluidic platforms have been reported for LCP crystallization.[11] Both platforms rely on complex operation strategies and have a number of limitations due to the difficulties of manipulating viscoelastic materials in microscale compartments.

Microfluidic Chip for LCP Crystallization. Here we present a microfluidic chip that combines LCP crystallization capabilities with X-ray transparency in a simple design that only requires a vacuum pump to introduce reagents. In the 12-well chip (Figure 1A), each well relies on diffusion to mix 60 nL of protein solution, 10.5 nL of dry lipid for mesophase formulation, and 244 nL of precipitant solution to induce crystallization. *The protein solution is layered on top of the lipid* (Figure 2A,B), *significantly reducing the diffusional path and, consequently, the mixing time compared to the traditional side-by-side placement of microfluidic compartments.*[10g,k,12] The chip screens two crystallization conditions in parallel and can be easily modified for more extensive screening.

For X-ray transparency, the chip is assembled from four polymeric layers with a combined thickness of only ∼200 μm.[10k] Fluid manipulation in the chip relies on channels and compartments patterned in two layers of elastomeric polydimethylsiloxane (PDMS) (Figure 1B,C). Top and bottom cyclic olefin copolymer (COC) layers (Figure 1C) impart rigidity and serve as as a barrier against water evaporation. Fluid flow and compartment filling in the PDMS fluid layer is achieved by applying negative pressure (vacuum) to microfluidic control lines in the PDMS control layer (Figures 1B,C and 2A−E).

To fabricate the chip, the PDMS fluid and control layers are patterned and sealed irreversibly with each other and the top
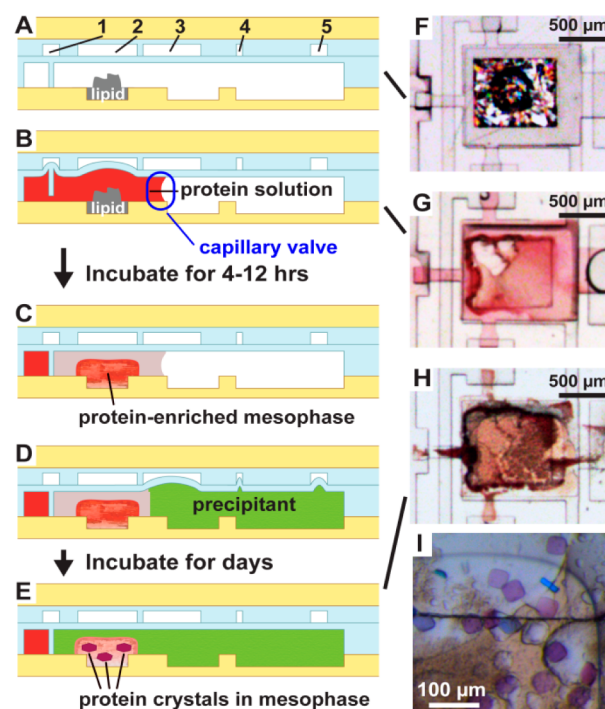

Figure 2. (A−E) Sequence of steps in the LCP protein crystallization protocol on-chip; (F−H) corresponding optical micrographs of the mesophase chamber. (A,F) The hybrid COC/PDMS/PDMS assembly is placed on the COC substrate prefilled with lipid. COC, yellow; PDMS, blue; lipid, gray. (B) Protein solution is combined with the lipid through the corresponding fluid line by applying negative pressure (vacuum) to control lines 1 and 2. (C) Protein-enriched mesophase forms spontaneously upon incubation, and (D) precipitant is introduced by applying negative pressure to control lines 3, 4, and 5. Line 2 in panel B and lines 3 and 5 in panel D serve to increase the rate of air withdrawal from their respective sample chambers. (E,H) Protein crystals form in the mesophase after incubation. (I) Representative example of RC crystals grown on-chip.

COC layer. For crystallization experiments, the 3-layer assembly is reversibly sealed, exploiting the adhesive properties of PDMS,[10k] to the COC bottom substrate containing solid lipid (Figures 2A and S3, Supporting Information). Further

detail on the fabrication procedure is provided in the Supporting Information (Figures S1−S3).

On-Chip Crystallization Protocol. The on-chip crystallization protocol follows the recently introduced LCP crystallization variant.[13] First, an auxiliary microfluidic assembly is used to fill designated compartments of the bottom COC substrate with lipid (Figure S2, Supporting Information). The auxiliary microfluidic chip is then removed, and the 3-layer assembly is placed on the bottom COC substrate prefilled with lipid (Figure 2A). Through a single inlet (Figure 1A), the protein solution is introduced into the 12 crystallization wells and is thus brought in contact with the lipid (Figure 2B,C). In the crystallization compartment only the area above the lipid, the mesophase chamber (Figure 1B), is filled. Filling of the rest of the crystallization well with protein solution is prevented by a capillary valve geometry[14] (obtained by appropriate choice of channel dimensions and wall angles) between the mesophase and the precipitant chambers (Figure 1B). Incubation of the protein solution with the lipid results in spontaneous formation of the protein-enriched mesophase[13,15] (Figure 2C). After several hours, precipitant solution is introduced, with the mesophase staying in place due to its high viscosity[16] (Figure 2D). Under favorable conditions, incubation of the precipitant with the protein-enriched mesophase results in crystal formation in the mesophase (Figure 2E,I).

Validation of On-Chip Crystallization and X-ray Diffraction Data Collection. We validated our approach by crystallizing photosynthetic reaction center (RC), a membrane protein from *Rhodobacter sphaeroides*, using previously reported crystallization conditions[13] to obtain crystals of up to 80 μm in size (Figure 2I). We collected X-ray diffraction data at room temperature (RT) from crystals in the chips ("on-chip") and solved the crystal structure of RC to a resolution of 2.5 Å (Table S1, Supporting Information). The chips were mounted directly, without modification, on the goniometer at beamline 21-ID-F at the Advanced Photon Source (APS), Argonne National Lab (ANL) (Figure 3A). Diffraction data from the crystals were easily resolved (Figure 3C), despite background scattering from chip materials (Figure S4, Supporting Information). The excellent optical properties of the chips facilitated crystal targeting during data collection (Figure 3A,B). In contrast, crystals grown in parallel using the classical LCP method in microplates (see Supporting Information) were difficult to locate in standard loop mounts because of the opacity of the mesophase (Figure S5, Supporting Information).[6,17]

Following our previously developed on-chip data collection strategy,[10k,12d] small wedges of data from multiple crystals were collected and merged into a single data set for building electron density maps. The ease of growing and analyzing multiple (tens to hundreds) isomorphous crystals in a single chip enables data collection under ambient conditions with minimal radiation damage effects. In contrast, traditional crystallographic protocols rely on the harvesting and mounting of a single crystal at a time, followed by the analysis of that crystal under cryogenic conditions to minimize radiation damage.[18] The challenges associated with this one-at-a-time manual protocol render analysis of multiple LCP-grown crystals at ambient conditions impractical.

Although RC crystallization conditions likely produce a sponge phase rather than a true LCP,[19] the term "LCP crystallization of proteins" is commonly used regardless of the
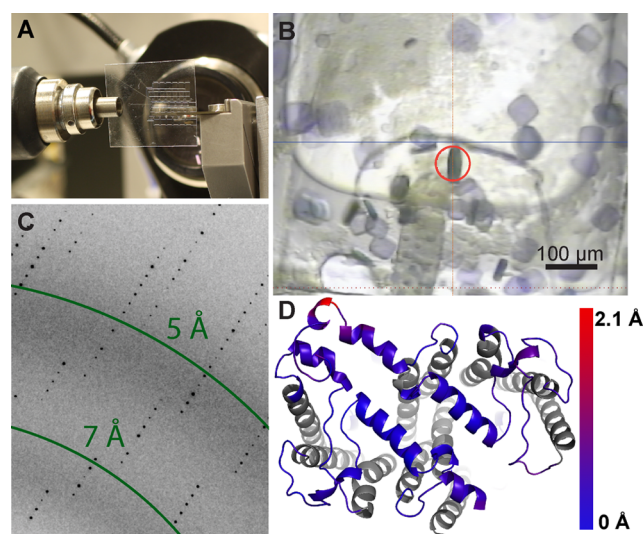

Figure 3. (A) Optical micrograph of an X-ray transparent chip for LCP crystallization mounted on beamline 21-ID-F at LS-CAT, ANL. (B) Section of a crystallization well with crystals as seen in the on-axis video microscope during X-ray data collection. The red circle represents the location and the footprint of the 50 μm X-ray beam. (C) Example of X-ray diffraction data from an RC crystal on-chip at RT. (D) rmsd visualization along the periplasmic side of our RT structure and a cryogenic structure (PDB ID: 2GNU). Residues in gray were not included in calculation. Image was generated using the ColorByRMSD script in PyMOL.[24]

exact mesophase type formed under specific crystallization conditions and is also adopted throughout this communication.

On-Chip RC Crystal Structure. The structure determined from on-chip data (Table S1, Supporting Information) agreed well with previously published structures of LCP-crystallized RC obtained using the traditional crystallization and data collection approach (PDB ID: 2GNU[20] and 1OGV[21]). The merged data set for our structure was complete (Table S1, Supporting Information), indicating that on-chip crystals were oriented randomly. Our RC structure was isomorphous with the structures reported previously[20,21] and had comparable structural statistics, refinement parameters, and final structural resolution. Values for R_{sym} and I/σ for the on-chip structure were typical of good diffraction data.

We also observed several important differences between cryogenic structures of RC[20,21] and our RT structure. First, the lattice parameters of our RC structure were up to 1.8% larger than those reported previously, indicating unit cell contraction upon flash cooling. Second, the mosaicity (long-range order) of crystals analyzed on-chip was nearly an order of magnitude lower (better order) compared to other high-resolution RC structures crystallized in LCP.[20,21] The higher mosaicity (poorer order) is typically related to the unit cell contraction caused by flash-cooling to cryogenic temperatures.[22] The availability of low-mosaicity crystals and noncryogenic data collection facilitated by the on-chip approach reported here may be highly beneficial for time-resolved protein crystallography.[23]

Root mean square deviation (rmsd) comparisons revealed noticeable nonuniformly distributed deviations in the positions of backbone alpha-carbons in our RC structure compared to both available cryo-structures[20,21] (Figure 3D and Table S2, Supporting Information). The greatest deviations were located along the hydrophilic chains at the periplasmic and cytosolic

sides of the protein (rmsd = 0.45 Å; Table S2, Supporting Information) and were as large as 2 Å at residues 268−271 of the L-subunit (Figures 3D and S6, Supporting Information). The hydrophobic chains embedded within the lipid bilayer showed a significantly smaller deviation (rmsd = 0.28 Å; Table S2, Supporting Information). Conversely, the rmsd values for superimposed cryogenic RC structures did not exceed 0.23 Å anywhere (Table S2, Supporting Information). The overall rmsd of 0.36−0.37 Å between the RT and the cryogenic structures was in the range reported for independent structure determinations of an identical protein[25] (Table S1, Supporting Information).

For soluble proteins, cryo-cooling has been shown to affect mechanistically relevant side-chain conformations and, in extreme cases, backbone conformations.[22] Similar analyses for LCP-crystallized membrane proteins are largely unavailable because of the difficulties of obtaining RT crystal structures that require screening of a larger number of crystals, as highlighted in the impressive recent studies of human membrane proteins under noncryogenic conditions.[26] While the transmembrane chains of the proteins are likely to be constrained by the membrane-like LCP environment, hydrophilic segments may undergo significant conformational changes upon flash-cooling, as also observed by Liu et al.[26a] These changes may be of importance for mechanistic studies and for protein docking, and the analysis of LCP-grown crystals under near-physiological temperatures, as enabled by our on-chip approach, may provide new insights into these phenomena.

In summary, we demonstrated the first X-ray transparent microfluidic chip for LCP crystallization of membrane proteins and subsequent on-chip X-ray diffraction data collection of multiple crystals on a single chip at room temperature for protein structure determination. We validated our approach by crystallizing a membrane protein and photosynthetic reaction center and solving its structure to a resolution of 2.5 Å. The chip automates metering and sample formulation, eliminates manual mesophase handling, and reduces the amount of sample per trial ∼7-fold compared to similar macroscale protocols,[13,15] and ∼3-fold compared to standard protocols with premixed mesophase.[2,3] In situ X-ray data collection on multiple crystals obviates cumbersome manual harvesting of fragile protein crystals. These features make our chips a valuable tool for the analysis of membrane proteins by providing a facile route to crystal structures and potentially to time-resolved studies of LCP-embedded proteins. For example, our on-chip analysis of RC revealed conformational flexibility in its hydrophilic chains at RT.

ASSOCIATED CONTENT

Ⓢ Supporting Information
Chip fabrication and operation, materials, X-ray analysis, background scattering, and rmsd analysis. This material is available free of charge via the Internet at http://pubs.acs.org.

AUTHOR INFORMATION

Corresponding Author
*(P.J.A.K.) E-mail: kenis@illinois.edu.

Author Contributions
§(D.S.K. and J.M.S.) These authors contributed equally to this work.

Notes
The authors declare no competing financial interest.

ACKNOWLEDGMENTS

REFERENCES

(1) Overington, J. P.; Al-Lazikani, B.; Hopkins, A. L. *Nat. Rev. Drug Discovery* **2006**, *5*, 993.

(2) Caffrey, M.; Cherezov, V. *Nat. Protocols* **2009**, *4*, 706.

(3) Katritch, V.; Cherezov, V.; Stevens, R. C. *Trends Pharmacol. Sci.* **2012**, *33*, 17.

(4) Caffrey, M.; Lyons, J.; Smyth, T.; Hart, D. J. In *Current Topics in Membranes*; Larry, D., Ed.; Academic Press: New York, 2009; Vol. *63*, p 83.

(5) Lynch, M. L.; Spicer, P. T., Eds. *Bicontinuous Liquid Crystals*; CRC Press: Boca Raton, FL, 2005; Vol. *127*.

(6) Cherezov, V.; Abola, E.; Stevens, R. C. *Methods Mol. Biol.* **2010**, *654*, 141.

(7) Cherezov, V. *Curr. Opin. Struct. Biol.* **2011**, *21*, 559.

(8) Cherezov, V.; Peddi, A.; Muthusubramaniam, L.; Zheng, Y. F.; Caffrey, M. *Acta Crystallogr., Sect. D: Biol. Crystallogr.* **2004**, *60*, 1795.

(9) (a) Cole, M. C.; Desai, A. V.; Kenis, P. J. A. *Sens. Actuators, B* **2011**, *151*, 384. (b) Stojanoff, V.; Jakoncic, J.; Oren, D. A.; Nagarajan, V.; Navarro Poulsen, J.-C.; Adams-Cioaba, M. A.; Bergfors, T.; Sommer, M. O. A. *Acta Crystallogr., Sect. F: Struct. Biol. Cryst. Commun.* **2011**, *67*, 971. (c) Hsin-Jui, W.; Basta, T.; Morphew, M.; Rees, D. C.; Stowell, M. H. B.; Lee, Y. C. *2013 8th IEEE International Conference on NEMS*, 2013; p 84. (d) Pinker, F.; Brun, M.; Morin, P.; Deman, A.-L.; Chateaux, J.-F.; Oliéric, V.; Stirnimann, C.; Lorber, B.; Terrier, N.; Ferrigno, R.; Sauter, C. *Cryst. Growth Des.* **2013**, *13*, 3333.

(10) (a) Kisselman, G.; Qiu, W.; Romanov, V.; Thompson, C. M.; Lam, R.; Battaile, K. P.; Pai, E. F.; Chirgadze, N. Y. *Acta Crystallogr., Sect. D: Biol. Crystallogr.* **2011**, *67*, 533. (b) Huh, D.; Hamilton, G. A.; Ingber, D. E. *Trends Cell Biol.* **2011**, *21*, 745. (c) Gerdts, C. J.; Elliott, M.; Lovell, S.; Mixon, M. B.; Napuli, A. J.; Staker, B. L.; Nollert, P.; Stewart, L. *Acta Crystallogr., Sect. D: Biol. Crystallogr.* **2008**, *64*, 1116. (d) Steinert, C. P.; Mueller-Dieckmann, J.; Weiss, M.; Roessle, M.; Zengerle, R.; Koltay, P. In *20th IEEE Intl. Conf. on MEMS*, Hyogo, Japan, 2007; p 561. (e) Ng, J. D.; Clark, P. J.; Stevens, R. C.; Kuhn, P. *Acta Crystallogr., Sect. D: Biol. Crystallogr.* **2008**, *64*, 189. (f) Dhouib, K.; Khan Malek, C.; Pfleging, W.; Gauthier-Manuel, B.; Duffait, R.; Thuillier, G.; Ferrigno, R.; Jacquamet, L.; Ohana, J.; Ferrer, J.-L.; Theobald-Dietrich, A.; Giege, R.; Lorber, B.; Sauter, C. *Lab Chip* **2009**, *9*, 1412. (g) Lin, W.-Y.; Wang, Y.; Wang, S.; Tseng, H.-R. *Nano Today* **2009**, *4*, 470. (h) Sauter, C.; Dhouib, K.; Lorber, B. *Cryst. Growth Des.* **2007**, *7*, 2247. (i) Greaves, E. D.; Manz, A. *Lab Chip* **2005**, *5*, 382. (j) Barrett, R.; Faucon, M.; Lopez, J.; Cristobal, G.; Destremaut, F.; Dodge, A.; Guillot, P.; Laval, P.; Masselon, C.; Salmon, J.-B. *Lab Chip* **2006**, *6*, 494. (k) Guha, S.; Perry, S. L.; Pawate, A. S.; Kenis, P. J. A. *Sens. Actuators, B* **2012**, *174*, 1.

(11) (a) Stroock, A. D.; Dertinger, S. K. W.; Ajdari, A.; Mezić, I.; Stone, H. A.; Whitesides, G. M. *Science* **2002**, *295*, 647. (b) Li, L.; Fu, Q.; Kors, C.; Stewart, L.; Nollert, P.; Laible, P.; Ismagilov, R. *Microfluid. Nanofluid.* **2010**, *8*, 789.

(12) (a) Zhong, J. F.; Chen, Y.; Marcus, J. S.; Scherer, A.; Quake, S. R.; Taylor, C. R.; Weiner, L. P. *Lab Chip* **2008**, *8*, 68. (b) Kang, L.; Chung, B. G.; Langer, R.; Khademhosseini, A. *Drug Discovery Today* **2008**, *13*, 1. (c) Hansen, C. L.; Sommer, M. O. A.; Quake, S. R. *Proc. Natl. Acad. Sci. U.S.A.* **2004**, *101*, 14431. (d) Perry, S. L.; Guha, S.;

Pawate, A. S.; Bhaskarla, A.; Agarwal, V.; Nair, S. N.; Kenis, P. J. A. *Lab Chip* **2013**, *13*, 3183.

(13) Wallace, E.; Dranow, D.; Laible, P. D.; Christensen, J.; Nollert, P. *PLoS One* **2011**, *6*, e24488.

(14) Moore, J.; McCuiston, A.; Mittendorf, I.; Ottway, R.; Johnson, R. *Microfluid. Nanofluid.* **2011**, *10*, 877.

(15) Kubicek, J.; Schlesinger, R.; Baeken, C.; Büldt, G.; Schäfer, F.; Labahn, J. *PLoS One* **2012**, *7*, e35458.

(16) Mezzenga, R.; Meyer, C.; Servais, C.; Romoscanu, A. I.; Sagalowicz, L.; Hayward, R. C. *Langmuir* **2005**, *21*, 3322.

(17) Kissick, D. J.; Gualtieri, E. J.; Simpson, G. J.; Cherezov, V. *Anal. Chem.* **2009**, *82*, 491.

(18) Garman, E. *Acta Crystallogr., Sect. D: Biol. Crystallogr.* **2010**, *66*, 339.

(19) Cherezov, V.; Clogston, J.; Papiz, M. Z.; Caffrey, M. *J. Mol. Biol.* **2006**, *357*, 1605.

(20) Wadsten, P.; Wöhri, A. B.; Snijder, A.; Katona, G.; Gardiner, A. T.; Cogdell, R. J.; Neutze, R.; Engström, S. *J. Mol. Biol.* **2006**, *364*, 44.

(21) Katona, G.; Andréasson, U.; Landau, E. M.; Andréasson, L.-E.; Neutze, R. *J. Mol. Biol.* **2003**, *331*, 681.

(22) (a) Dunlop, K. V.; Irvin, R. T.; Hazes, B. *Acta Crystallogr., Sect. D: Biol. Crystallogr.* **2004**, *61*, 80. (b) Fraser, J. S.; van den Bedem, H.; Samelson, A. J.; Lang, P. T.; Holton, J. M.; Echols, N.; Alber, T. *Proc. Natl. Acad. Sci. U.S.A.* **2011**, *108*, 16247.

(23) Ren, Z.; Moffat, K. *J. Synchrotron Radiat.* **1994**, *1*, 78.

(24) *PyMOL*; Schrodinger, LLC: New York, 2010.

(25) Carugo, O. *J. Appl. Crystallogr.* **2003**, *36*, 125.

(26) (a) Liu, W.; Wacker, D.; Gati, C.; Han, G. W.; James, D.; Wang, D.; Nelson, G.; Weierstall, U.; Katritch, V.; Barty, A.; Zatsepin, N. A.; Li, D.; Messerschmidt, M.; Boutet, S.; Williams, G. J.; Koglin, J. E.; Seibert, M. M.; Wang, C.; Shah, S. T. A.; Basu, S.; Fromme, R.; Kupitz, C.; Rendek, K. N.; Grotjohann, I.; Fromme, P.; Kirian, R. A.; Beyerlein, K. R.; White, T. A.; Chapman, H. N.; Caffrey, M.; Spence, J. C. H.; Stevens, R. C.; Cherezov, V. *Science* **2013**, *342*, 1521. (b) Weierstall, U.; James, D. I.; Wang, C.; White, T. A.; Wang, D.; Liu, W.; Spence, J. C. H.; Doak, R. B.; Nelson, G.; Fromme, P.; Fromme, R.; Grotjohann, I.; Kupitz, C.; Zatsepin, N. A.; Liu, H.; Basu, S.; Wacker, D.; Won Han, G.; Katritch, V.; Boutet, S.; Messerschmidt, M.; Williams, G. J.; Koglin, J. E.; Seibert, M. M.; Klinker, M.; Gati, C.; Shoeman, R. L.; Barty, A.; Chapman, H. N.; Kirian, R. A.; Beyerlein, K. R.; Stevens, R. C.; Li, D.; Shah, S. T. A.; Howe, N.; Caffrey, M.; Cherezov, V. *Nat. Commun.* **2014**, *5*, 3309.